PHYSICAL REVIEW A **79**, 050702(R) (2009)

Inelastic titanium-titanium collisions

Mei-Ju Lu, Vijay Singh, and Jonathan D. Weinstein*
Department of Physics, University of Nevada, Reno, Nevada 89557, USA
(Received 26 December 2008; revised manuscript received 27 March 2009; published 26 May 2009)

We have measured cold inelastic collisions between neutral ground-state titanium atoms: collisions that cause transitions between the different magnetic sublevels of the $[3d^24s^2]^3F_2$ ground state of ^{50}Ti, as well as collisions that cause transitions between the fine-structure levels of the $[3d^24s^2]^3F_J$ electronic ground state. Both processes occur with large rate coefficients, as would be expected from titanium's anisotropic electronic potential.

DOI: 10.1103/PhysRevA.79.050702 PACS number(s): 34.50.−s, 37.10.De

Atoms with nonzero orbital angular momentum ($L>0$) have an anisotropic electrostatic interaction potential, which is expected to lead to large inelastic collision cross sections [1,2]. Previously, collisions between atoms with fine structure have been studied at elevated temperatures due to their importance in the terrestrial atmosphere [3,4]. Recently, these collisions have become of interest again due to their promise of interesting many-body behavior and the potential to create new types of quantum fluids [5–10]. This promise, along with the development of new methods to cool and trap atoms with $L>0$, has sparked interest in investigating their collisional properties [11–13]. Understanding the nature of these collisional interactions is crucial for realizing new regimes of anisotropically interacting quantum degenerate gases.

Recent experiments with metastable alkaline-earth-metal-like atoms observed large inelastic collision rates at ultracold temperatures. Hemmerich *et al.* [11] measured a magnetic trap loss rate constant of around 3×10^{-10} cm^3 s^{-1} for metastable $[4s4p]^3P_2$ calcium atoms. The trap loss is due to the combined contribution of Zeeman relaxation collisions (m-changing collisions), fine-structure relaxation collisions (J-changing collisions), and electronic-state changing collisions (de-excitation of the metastable state of calcium). Yamaguchi *et al.* [12] measured inelastic collisions between (unpolarized) metastable $[4f^{14}6s6p]^3P_2$ ytterbium atoms in an optical trap and found an inelastic collision rate constant of $1.0(3)\times10^{-11}$ cm^3 s^{-1}.

In this work, we measure the inelastic collision properties of ground-electronic-state atomic titanium for J-changing and m-changing collisions. By working with ground-state atoms we can ensure there is no contribution to collision rates from electronic quenching conditions, which have been measured to be significant for metastable alkaline earth metals [13].

The ground electronic state of titanium is $[3d^24s^2]^3F_J$, with $J=2$, 3, and 4. Recent experiments measuring collisions between titanium and a structureless collision partner (helium) observed a dramatic suppression of m-changing collisions [14,15] and J-changing collisions [16] due to titanium's submerged shell structure. This suppression effect is not unique to titanium and has been observed to hold for a wide variety of submerged-shell atoms colliding with helium [17]. It has been suggested that the submerged shell might similarly suppress inelastic collisions between atoms with orbital angular momentum [15]; whether this is true is important for determining the efficiency of evaporative cooling in magnetic traps.

Our experimental apparatus and diagnostic techniques are similar to those described in Ref. [16]. Briefly, we laser ablate a titanium plate to produce titanium atoms. We use a cryogenic helium buffer gas to cool the titanium atoms. We use laser absorption spectroscopy on the $[3d^24s^2]a\ ^3F_J\rightarrow[3d^24s4p]y\ ^3F_J$ transitions at 399 nm to state-selectively monitor them. To measure inelastic collisions, we perturb the internal-state distribution of our titanium atoms by optical pumping [18]. By monitoring the return of the atomic populations to thermal equilibrium, we determine inelastic collision rates.

In this experiment, we work with natural abundance titanium and spectroscopically resolve the ^{50}Ti isotope to optically pump it and to measure ^{50}Ti-Ti collisions. ^{50}Ti is an $I=0$ nucleus and consequently has no hyperfine structure. Its natural abundance is 5.4% [19].

The key to measuring ^{50}Ti-Ti collisions is obtaining a large density of atomic titanium. We are able to generate atom densities on the order of 10^{12} cm^{-3}, numbers on the order of 10^{15} and optical densities (ODs)>300. The ability to generate large densities and numbers of atoms at cryogenic temperatures is of interest for improving the performance of atomic magnetometers [20]. The ability to generate large optical densities is of interest for slow-light experiments [21]. We note our density, number, and OD exceed those previously reported at cryogenic temperatures [20,21]. While the different production efficiencies may be due to the species studied, we suspect the size of the cryogenic cell plays a role in atom production efficiency. Our cryogenic cell is roughly 10 cm in size, while the cells of Refs. [20,21] are roughly 2 cm. A larger cell ensures atoms are stopped and thermalized before they traverse the cell even at low helium densities; operating at low helium density may be favorable for ablation efficiency. On a separate note, a larger cell also provides longer diffusion times, which may be advantageous for a variety of experiments. For the range of helium densities employed in the current work, the exponential lifetime varies from 25 to 120 ms.

To measure m-changing collisions between $^3F_2$ titanium

*weinstein@physics.unr.edu

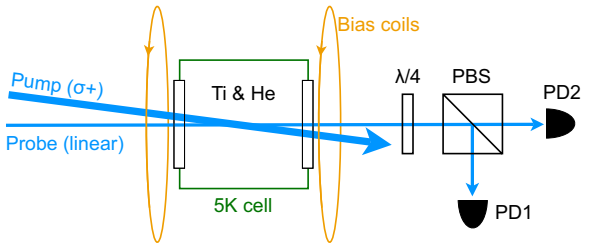

FIG. 1. (Color online) Experimental setup for measuring ^{50}Ti polarization, as described in the text. Typical probe powers are on the order of 1 μW, typical pump powers are on the order of a few mW. The angle between pump and probe is exaggerated for clarity. A typical probe beam diameter is 3 mm; a typical pump beam diameter is 3 cm. Photodiodes PD1 and PD2 monitor the absorptions of σ^+ and σ^- light.

atoms, we generate a magnetic field with a pair of Helmholtz coils to split the degeneracies of the m_J levels and define a polarization axis. Under our experimental conditions, the temperature is very large compared to the Zeeman splitting. In thermal equilibrium, the sample is essentially unpolarized. To induce a polarization, we send a pulse of circularly polarized light along the field to optically pump the m states of ^{50}Ti. We probe the evolution of the ^{50}Ti polarization by measuring the relative absorption of σ^+ and σ^- light from a linearly polarized probe beam, as shown in Fig. 1.

By fitting the return to equilibrium, as shown in Fig. 2, we determine the m relaxation rate, $1/\tau$. We measure this rate as a function of titanium density. As seen in Fig. 3, $1/\tau$ increases linearly with ^{48}Ti optical density; from its dependence on the titanium density we determine the ^{50}Ti-Ti collision rate. To verify that we are measuring ^{50}Ti-Ti collisions, we perform a series of systematic checks, discussed below.

To measure J-changing collisions, we optical pump atoms from the $^3F_2$ ground state to the $^3F_3$ ground state, 170 cm^{-1} above the $^3F_2$ [19]. We observe their return to equilibrium by absorption spectroscopy, as described at greater length in Ref. [16].

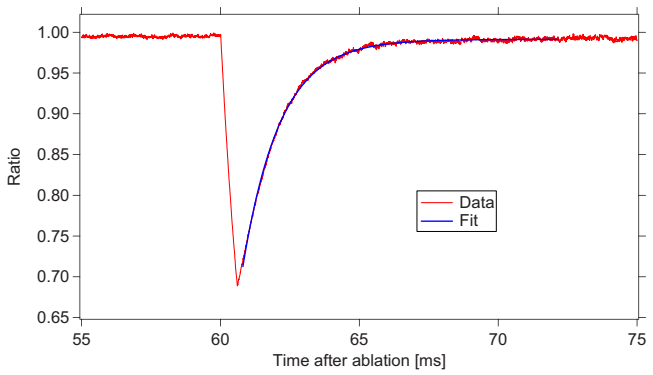

FIG. 2. (Color online) ^{50}Ti polarization, as monitored by the ratio of the optical densities for σ^+ and σ^-. The optical pumping beam is on from 60.0 ms to 60.6 ms; time is measured relative to the ablation pulse. Prior to the pumping beam, there is little polarization in the atomic sample and a small polarization is induced by the pumping beam. We fit the return to equilibrium to $e^{-t/\tau}$ to determine $1/\tau$, the decay rate of ^{50}Ti polarization.

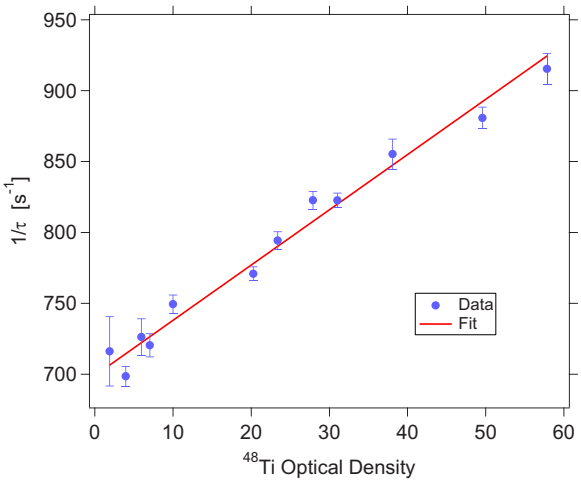

FIG. 3. (Color online) $1/\tau$, the decay rate of ^{50}Ti polarization, plotted vs ^{48}Ti optical density, at a temperature of 5 K and helium density 6.6×10^{15} cm^{-3}. Error bars are from statistical error; there is an additional uncertainty in the OD of $\pm10\%$. The offset is due to ^{50}Ti-He collisions, which occur with a rate coefficient of $(1.2\pm0.6)\times10^{-13}$ cm^3 s^{-1} [16]. The slope is due to ^{50}Ti-Ti collisions.

To determine the Ti–Ti collision rate coefficient $k=\frac{1}{\pi n}$, we need to know the density of titanium atoms n within our cell. To determine the density distribution, we use absorption spectroscopy to image the atoms. At early times after laser ablation, the distribution of atoms is complicated and difficult to model. Fortunately, as shown in Fig. 4, the distribution quickly evolves into a simple one which is well approximated by the lowest-order diffusion mode of our nearly-rectangular cell: a simple cosine distribution [22]. We restrict our analysis to experimental conditions which are well approximated by this diffusion model.

How to calculate collision rates in the presence of an inhomogeneous density distribution is well understood from experimental studies of collisions inside traps [23]. However, those experiments are typically conducted in a regime where the motion of atoms through the trap volume is very fast

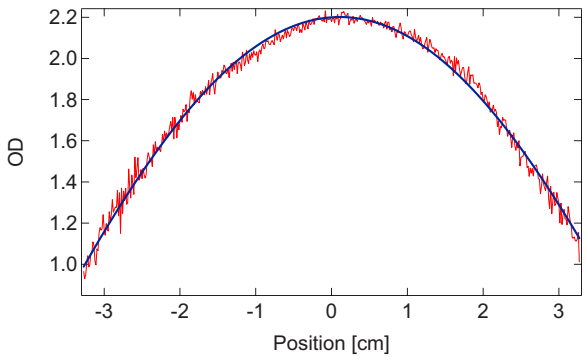

FIG. 4. (Color online) Measured density distribution within the cell, along with a fit to the lowest-order diffusion mode of a rectangular cell [22]. Position is measured along the probe beam: the zero is the center of the cell, and the cell walls (windows) are at ±5.1 cm. The measurement was taken 15 ms after a 0.1 J ablation pulse at a helium density of 1.7×10^{16} cm^{-3}.

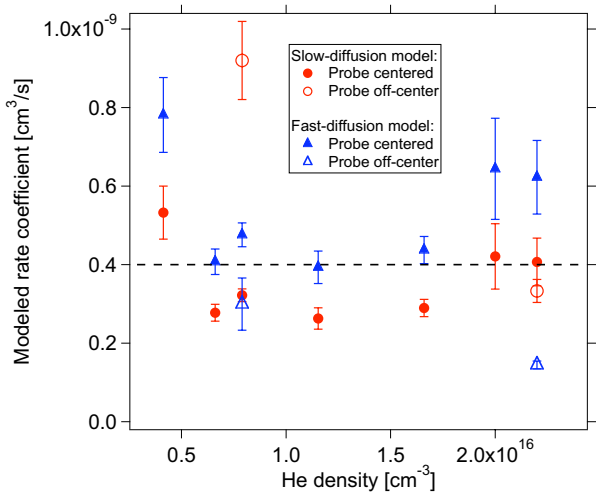

FIG. 5. (Color online) Rate constants from the fast-diffusion (triangle) and slow-diffusion (circle) models. Solid symbols were obtained with the probe beam traversing the cell near its center. The hollow symbols are from an off-center probe beam. We note that the two models give quite different results with an off-center probe beam, but the fast-diffusion model at low helium density shows agreement with the slow-diffusion model at high helium density. The dotted line indicates our value for the *m*-changing rate coefficient.

compared to the inelastic collision rate. Due to the slow diffusive motion of the titanium atoms through the helium, our data are not always obtained in that limit.

Consequently, we calculate the inelastic collision rate in two limiting cases. In the first case, we assume the atoms move very fast compared to the inelastic collision rate, in which case the rate constant is calculated by a weighted average of the atom density over the entire cell volume. In the second case, in which we assume the atoms move very slowly compared to the inelastic collision rate, the rate constant was calculated by a weighted average of the atom density over the region within the probe beam. We note that low-helium-pressure data analyzed under the "fast-diffusion" model show good agreement with high-helium-pressure data analyzed under the "slow-diffusion" model, as shown in Fig. 5. Because much of our data are obtained in an intermediate regime, our experimental error is dominated by our modeling error, which we estimate from the discrepancies between the two limiting case models. Our measured values are listed in Table I. We measured *m* relaxation at fields of 3 and 6 G, and no difference was observed in the inelastic collision rate to within our experimental error.

To check for systematics and to verify that we are measuring Ti–Ti collisions, we vary our experimental parameters

TABLE I. 5 K ^{50}Ti-Ti inelastic collision rate coefficients and thermally averaged scattering cross sections [22].

	k ($\mathrm{cm^3\ s^{-1}}$)	$\bar{\sigma}$ ($\mathrm{cm^2}$)
J-changing	$(1.5 \pm 0.7) \times 10^{-10}$	$(2.3 \pm 1.0) \times 10^{-14}$
m-changing	$(4.0 \pm 1.2) \times 10^{-10}$	$(6.1 \pm 1.8) \times 10^{-14}$

to confirm that k has no dependence on them. We vary the ablation energy from roughly 30 to 120 mJ [24], and we vary the helium density over a range from 4×10^{15} to 2.2×10^{16} $\mathrm{cm^{-3}}$ [25] and obtain consistent values for k. We vary the time at which we optically pump atoms over a range from 10 to 160 ms following the ablation pulse [26] and find consistent values for k.

It is likely that we produce other species (such as dimers or clusters) during the laser ablation. However, the dimer and cluster production efficiency are expected to vary strongly with ablation energy and buffer gas density [27], and any clusters produced are likely to have a different diffusion time scale than titanium atoms. Consequently, because the measured value of k is observed to be independent of the ablation energy, helium density, and measurement time, we are confident that we are measuring collisions with titanium atoms and not collisions with other products of ablation.

In conclusion, we have measured ^{50}Ti-Ti inelastic collisions at 5 K. We note that the measured ^{50}Ti-Ti *m*-changing cross section is larger than the *J*-changing cross section, as one might expect from the (cross-species) measurements of Refs. [11,12]. Unlike titanium-helium collisions, which exhibit a large suppression of inelastic collisions due to the "submerged shell" structure of Ti, there is no evidence of such suppression in Ti–Ti collisions. This is similar to the measurements of Harris *et al.* in investigations of spin-exchange collisions in Mn (an $L=0$ atom, also measured at cryogenic temperatures). In Mn–Mn collisions, no evidence of suppression of inelastic collisions was seen due to Mn's submerged shell [28]. An open question is whether submerged-shell suppression of inelastic collisions [15,17] is unique to collisions with helium—perhaps because of its exceptionally weak interatomic interaction potentials—or whether the suppression effect exists generally for collisions with "structureless" $^1S_0$ collision partners.

The measured collisional cross sections are for ^{50}Ti colliding with natural abundance atomic titanium. It is important to note that in our measurements of *m* relaxation, the other isotopes of titanium are unpolarized. Consequently, the *m*-changing collisions may occur through spin exchange. However, we note the Ti–Ti inelastic cross section is larger than would be expected for spin-exchange collisions, which have typical cross sections on the order of 2×10^{-14} $\mathrm{cm^2}$ at elevated temperatures [29].

Similarly, it is possible that our *J*-changing collisions are mediated through a "spin anisotropy" term in their interaction potential [30]. Unambiguously discerning the contribution from spin anisotropy (which would not exist for a fully polarized sample) and the electronic-interaction anisotropy (which would always be present) would require a repetition of the experiment with a fully polarized Ti sample. Due to the very high optical density of the dominant isotope and our limited laser power for optical pumping, this is impractical with our current apparatus.

We note that these collisions were made with cold atoms but under conditions that are far from the asymptotic $T=0$ limit. We cannot extrapolate these measurements to predict Ti–Ti collisions in the threshold regime. However, we note that because the measured rates involve a thermal averaging

over multiple partial waves and a wide range of scattering phases, we expect the measured behavior to reflect the "generic" behavior of collisions between atoms with nonzero angular orbital momentum.

We thank Matthew P. Karam for technical assistance with our imaging system. This work was supported in part by a grant from the University of Nevada Reno, Junior Faculty Research Grant Fund.

[1] A. Derevianko, S. G. Porsev, S. Kotochigova, E. Tiesinga, and P. S. Julienne, Phys. Rev. Lett. **90**, 063002 (2003).
[2] V. Kokoouline, R. Santra, and C. H. Greene, Phys. Rev. Lett. **90**, 253201 (2003).
[3] B. Zygelman, A. Dalgarno, and R. D. Sharma, Phys. Rev. A **49**, 2587 (1994).
[4] B. Zygelman, A. Dalgarno, and R. D. Sharma, Phys. Rev. A **50**, 3920 (1994).
[5] L. Santos, G. V. Shlyapnikov, P. Zoller, and M. Lewenstein, Phys. Rev. Lett. **85**, 1791 (2000).
[6] K. Góral, L. Santos, and M. Lewenstein, Phys. Rev. Lett. **88**, 170406 (2002).
[7] J. Stuhler, A. Griesmaier, T. Koch, M. Fattori, T. Pfau, S. Giovanazzi, P. Pedri, and L. Santos, Phys. Rev. Lett. **95**, 150406 (2005).
[8] M. A. Baranov, Phys. Rep. **464**, 71 (2008).
[9] T. Lahaye, T. Koch, B. Frohlich, M. Fattori, J. Metz, A. Griesmaier, S. Giovanazzi, and T. Pfau, Nature (London) **448**, 672 (2007).
[10] K.-K. Ni, S. Ospelkaus, M. H. G. de Miranda, A. Pe'er, B. Neyenhuis, J. J. Zirbel, S. Kotochigova, P. S. Julienne, D. S. Jin, and J. Ye, Science **322**, 231 (2008).
[11] D. Hansen and A. Hemmerich, Phys. Rev. Lett. **96**, 073003 (2006).
[12] A. Yamaguchi, S. Uetake, D. Hashimoto, J. M. Doyle, and Y. Takahashi, Phys. Rev. Lett. **101**, 233002 (2008).
[13] A. Traverso, R. Chakraborty, Y. N. M. de Escobar, P. G. Mickelson, S. B. Nagel, M. Yan, and T. C. Killian, e-print arXiv:0809.0936v2.
[14] R. V. Krems, J. Klos, M. F. Rode, M. M. Szczesniak, G. Chalasinski, and A. Dalgarno, Phys. Rev. Lett. **94**, 013202 (2005).
[15] C. I. Hancox, S. C. Doret, M. T. Hummon, R. V. Krems, and J. M. Doyle, Phys. Rev. Lett. **94**, 013201 (2005).
[16] M.-J. Lu, K. S. Hardman, J. D. Weinstein, and B. Zygelman, Phys. Rev. A **77**, 060701(R) (2008).
[17] C. I. Hancox, S. C. Doret, M. T. Hummon, L. Luo, and J. Doyle, Nature (London) **431**, 281 (2004).
[18] A. Hatakeyama, K. Enomoto, and T. Yabuzaki, Phys. Scr., T **110**, 294 (2004).
[19] J. E. Sansonetti, W. C. Martin, and S. L. Young, *Handbook of Basic Atomic Spectroscopic Data* (NIST, Gaithersburg, Maryland, 2005); http://physics.nist.gov/PhysRefData/Handbook/
[20] A. O. Sushkov and D. Budker, Phys. Rev. A **77**, 042707 (2008).
[21] T. Hong, A. V. Gorshkov, D. Patterson, A. S. Zibrov, J. M. Doyle, M. D. Lukin, and M. Prentiss, Phys. Rev. A **79**, 013806 (2009).
[22] J. B. Hasted, *Physics of Atomic Collisions*, 2nd ed. (American Elsevier, New York, 1972).
[23] N. Masuhara, J. M. Doyle, J. C. Sandberg, D. Kleppner, T. J. Greytak, H. F. Hess, and G. P. Kochanski, Phys. Rev. Lett. **61**, 935 (1988).
[24] The minimum ablation energy is limited by our need to produce high titanium densities. The maximum is limited by the capabilities of our laser.
[25] The minimum helium density is limited due to poor titanium atom densities obtained at low helium pressure. The maximum helium density is limited by our restriction that the titanium distribution must fit well to the lowest-order diffusion mode, this is no longer the case at high helium pressures.
[26] We cannot measure collisions at earlier times because the density distribution has not yet reached the lowest mode and/or the absorption spectroscopy is saturated. At later times we can no longer measure Ti–Ti collisions due to low titanium atom density.
[27] A. D. Sappey and T. K. Gamble, Appl. Phys. B: Lasers Opt. **53**, 353 (1991).
[28] J. G. E. Harris, S. V. Nguyen, S. C. Doret, W. Ketterle, and J. M. Doyle, Phys. Rev. Lett. **99**, 223201 (2007).
[29] W. Happer, Rev. Mod. Phys. **44**, 169 (1972).
[30] R. Krems, G. C. Groenenboom, and A. Dalgarno, J. Phys. Chem. A **108**, 8941 (2004).